DETECTOR CHARACTERIZATION OF ADVANCED LIGO

By

Thomas J. Massinger

B.S. Physics, Utica College, Utica, NY 13502

Dissertation
Submitted in Partial Fulfillment of the Requirements
for the degree of
Doctor of Philosophy in Physics

Syracuse University
June 2016

DETECTOR CHARACTERIZATION OF ADVANCED LIGO

By

Thomas J. Massinger

B.S. Physics, Utica College, Utica, NY 13502

DISSERTATION
SUBMITTED IN PARTIAL FULFILLMENT OF THE REQUIREMENTS
FOR THE DEGREE OF
DOCTOR OF PHILOSOPHY IN PHYSICS

Syracuse University
June 2016

Approved : _____

Prof. Peter R. Saulson

Date : _____

ABSTRACT

Placeholder with reference (Sidles-Sigg instability [1]).

Contents

List of Tables

List of Figures

Preface

The work presented in this thesis stems from my participation in the LIGO Scientific Collaboration (LSC). This work does not reflect the scientific opinion of the LSC and it was not reviewed by the collaboration.

Acknowledgments

Thank you for the music.........

to diglett

Chapter 1

Introduction

The Advanced Laser Interferometer Gravitational-Wave Observatory (aLIGO) is part of an international effort to detect gravitational waves. The search will resume later this year with the two aLIGO sites in Washington and Louisiana, which will ramp up to full design sensitivity over the following few years.

1.1   Basic layout of aLIGO

In its simplest form, aLIGO is a Michelson interferometer with Fabry-Pérot cavities for arms (see figure 1). In each Fabry-Pérot cavity, the mirror closer to the Michelson beam splitter is called the input test mass (ITM) and the other mirror is called end test mass (ETM).

When a gravitational wave passes through the detector, it causes changes in the distance between the ETM and ITM in each cavity. Because the wave is quadrapolar, the changes in the x direction will have the opposite sign of the changes in the y direction. This causes a relative phase shift in each of the arms in opposite directions. When they recombine at the beam splitter, the phase shifts cause changes in the interference between the two beams, changing the amount of power at the the output port. We can detect these power fluctuations to reconstruct the phase shift and thus the strain, $h = \Delta L/L$ experienced by the interferometer due to the gravitational wave. We then use techniques like matched filtering to compare the strain signal from the interferometer to models of expected signals to search for events hidden in the noise background of the interferometer.
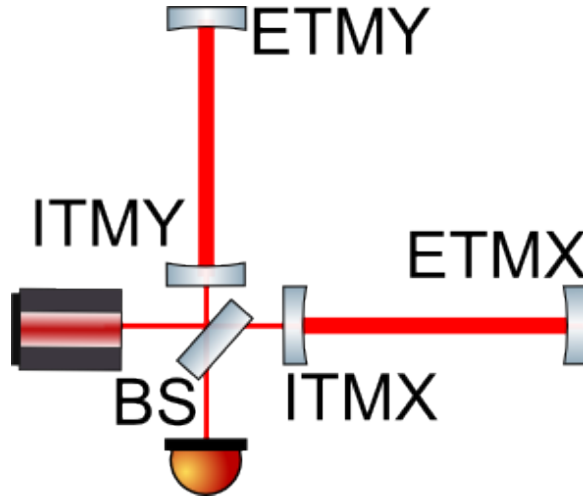
Figure 1 : In its simplest form, aLIGO is a Michelson interferometer with Fabry-Pérot cavities for arms. Light from the laser is split by the beam splitter (BS), then enters the arm cavities through the input test masses (ITMX and ITMY). Power builds up in the cavity between input and end test masses (ETMX and ETMY). When a gravitational wave passes through the detector, it shifts the phases of light in the two arms in opposite directions. Because the cavity is over-coupled ($r_{ITM} < r_{ETM}$), light leaves the arm cavities and goes back to the BS. The phase-shifted light from the two cavities interferes at the BS, producing the error signal that we measure with a photodiode.

Chapter 2

Instrumental Detector Characterization

I did a whole bunch of instrumental Detchar.

2.1 Analog-to-Digital Conversion

Advanced LIGO interferometers are controlled in real-time using a digital control system installed on a series of computers referred to as front end computers. This system overall is referred to as the Front End Control (FEC) subsection of the more expansive Control and Data System (CDS). In a control loop, the FE computers must be capable of reading in an analog signal from the interferometer (position measurements, error signals, coil currents, etc), digitally sampling that analog signal, using these now digital values in a series of control algorithms, and outputting an analog control signal to send back into the interferometer.

The process of digital sampling is handled by an analog-to-digital converter (ADC) and the process of analog output is handled by a digital-to-analog converter (DAC). Since these converters are linearly mapping a continuous signal onto a discrete range, they are limited by their digital bit depth. For example, a 16 bit ADC is only capable of representing 2^{16} discrete values, or a range from zero to 65536. This range is often centered around zero, giving the ADC the capability to handle a range of ± 32768. An incoming analog signal is mapped onto this range and converted into a digital signal.

For example, if I was sampling an analog signal with a range of $\pm 100V$, 100V would be mapped to 32768 and -100V would be mapped to -32768 with all of the intermediate voltage values being linearly mapped to the range. This means our digital system would recognize a discrete step size of $100/32768 \approx 3.05mV$.

2.2   Motivation

Looking at the system described above, we must be aware of how our system is going to react when our analog input signal exceeds the intended maximum value of 100V (e.g., a 110V input). The ADC has already assigned its maximum digital value to 100V. This is called range saturation. In this case the ADC will continuously output its maximum value as it has no way to map 110V into a discrete value. The same process can occur in a DAC when a digital signal is sent out at the maximum allowed digital value.

If the digital system is not able to correctly sample and understand an analog error signal, it is easy to imagine a scenario where the reponse of the digital system and the output control signal are not able to complete the control loop as designed. This may cause glitches or misalignments.

We must also consider the fact that many ADCs are calibrated to reflect the intended dynamic range of an optic. If a saturation is occurring, there is a good chance that an optic has moved beyond this intended dynamic range, which also may cause glitches or misalignments.

The ADCs and DACs are monitored by a series of auxiliary channels. The most useful channels are of the form:

```
L1:FEC-21_DAC_OVERFLOW_0_0
```

Parsing this channel name:

```
L1:FEC-{model number}_{ADC/DAC}_OVERFLOW_{ADC/DAC number}_{channel number}
```

These overflow monitor channels are cumulative. If the channel has no saturation at the time of sampling, the overflow channel's reported value will not increase. If the channel was saturated during the last sample, the value of the channel will increase in discrete steps equal in size to the maximum value of the channel.

Chapter 3

IMC Upconversion

3.1 Abstract

LIGO interferometers use several high finesse optical cavities for gravitational wave detection. The lengths of these cavities are controlled using radio frequency (RF) modulation-demodulation techniques in a Pound-Drever-Hall (PDH) locking scheme. This scheme provides a PDH error signal that is linear to cavity length over a specific range. This study examines the specific case of the triangular ring cavity uses in LIGO interferometers for input mode cleaning. When the length of the cavity approaches the boundaries of the PDH error signal linear range, our model of the input mode cleaner PDH response shows that the resulting error signal contains non-linear spectral artifacts. This model and understanding of the non-linear cavity responses will be useful in the commissioning phase of the Advanced LIGO project for more precisely locating and eliminating systematic noise sources in the interfereometers

3.2 Model

The PDH response of the cavity was modeled using measured values of optical reflectivity and free spectral range of the Livingston input mode cleaner. The input beam was the nominal LIGO carrier beam with a frequency of $\omega = 281.8$ THz ($\lambda = 1064$ nm) and modulation sidebands of $\Omega = \pm 24$ MHz.

The reflection coefficient of a LIGO input mode cleaner as a function of input beam frequency is given as,

$$F(\omega) = \frac{r(1 + e^{-i\phi})}{1 + r^2 e^{-i\phi}} = \frac{r(1 + e^{-i(\frac{\omega}{\nu_{fsr}})})}{1 + r^2 e^{-i(\frac{\omega}{\nu_{fsr}})}} \tag{3.1}$$

where r is the reflectivity of the input mirror, ϕ is the round-trip phase accumulated when traversing the cavity, and ν_{fsr} is the free spectral range of the cavity [2].

In a situation where the carrier beam is resonant in the cavity and the modulation sidebands are high enough in frequency that they are not resonant, the PDH error signal, here denoted ϵ is given as

$$\epsilon(\omega) = -2\sqrt{P_c P_s} \, \mathrm{Im}\{F(\omega)F^*(\omega + \Omega) - F^*(\omega)F(\omega - \Omega)\}, \tag{3.2}$$

where P_c is the the carrier beam power and P_s is the sideband power [3].

Note: the above error signal is a function of laser frequency. This is an artifact of the original intent of PDH locking: using a fixed length resonant cavity to control the frequency of a laser by forcing it to match the cavity length. We can apply the same technique but flip the direction of feedback and use a highly stable laser to control the length of a free swinging resonant cavity by pushing on the mirrors to match the cavity length to the laser wavelength. The laser frequency detuning and cavity length detuning are linearly mapped to one another using the free spectral range of the resonant cavity.

Importantly, this error signal is linear to the length of the IMC within a certain range of motion. If the optics begin swinging too far away from the nominal locking point, we will begin to see a non-linear response and eventually a lock loss.

To explore this non-linearity, we injected a sinusoidal cavity motion into our model and observed the resulting error signal.

We explored two specific cases. Figure 1 shows spectra of the injected sinusoidal cavity motion (green) and the resulting non-linear error signal (blue). This motion was injected asymetrically about the nominal cavity locking point ($\epsilon = 0$) and therefore we see both even and odd harmonics of the injection frequency.

Figure 2 shows spectra of the injected sinusoidal cavity motion (green) and the resulting non-linear error signal (blue). However, this time the motion was injected symetrically about the nominal cavity locking point and as a result we only see odd harmonics of the fundamental frequency.

We hope to use this model as an explanation of systematic noise found in the aLIGO IMC.

Figure 2 : Sinusoidal cavity motion with frequency 2.78 Hz injected asymmetrically about the locking point of the cavity results in a PDH error signal containing non-linear spectral artifacts at harmonics of the injected cavity motion.
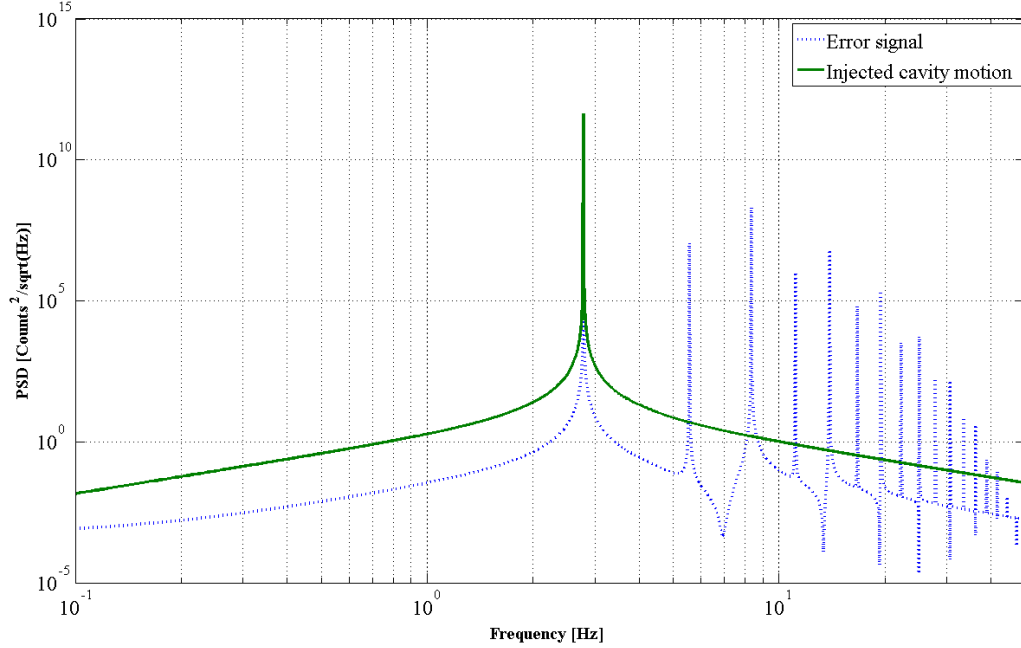

3.3   Upconversion noise in aLIGO

The aLIGO input mode cleaner (IMC) is a triangular ring cavity whose length is sensed and controlled using the PDH locking technique. Each of the three mirrors in the cavity is staged as the bottom mass of a triple suspension in order to passively isolate the mirrors from potential noise sources. In addition, the chambers holding the IMC mirrors are isolated from ground motion by two stages of active seismic isolation. This isolation, however, is not completely impervious to external excitations. During periods of time with excess ground motion we can see seismic noise coupling into the cavity length and its control signal.

Specifically, when we see excess seismic noise in the 1-5 Hz anthropogenic band (believed to be caused by a commercial railroad a few kilometers from the LIGO Livingston Laboratory), we see highly structured noise in the IMC control signal in

Figure 3 : If the motion is symmetric about the cavity locking point, we see only odd harmonics of the injection frequency.
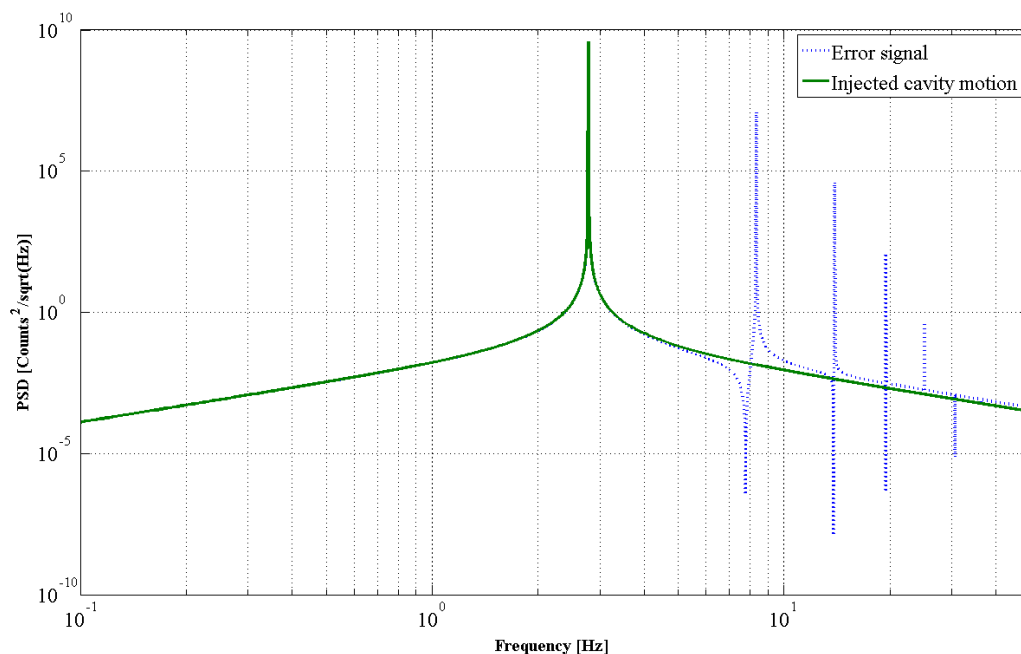

the 10-100 Hz band. This physical mechanism is consistent with the idea of a PDH range saturation. If excess seismic motion reaches the suspension and the optics begin swinging around, it's feasible that they could start to saturate the linear range of the PDH loop.

The noise takes a form very similar in structure to the non-linear PDH signal, displaying strong odd harmonics and weaker even harmonics. The IMC control signal has an associated noise floor that obscures parts of these peaks. The theoretical model uses sinusoids with a highly specified frequency and thus displays very sharp peaks in its spectrum. It should be noted that the peaks in the IMC control signal are the manifestation of a physical process, not digitally generated, and have some natural width to them.

3.4   Next steps

While we have demonstrated that this mechanism is a feasible explanation for the IMC upconversion noise, it has not yet been fully proven. We are currently looking

Figure 4 : Spectral comb with a fundamental frequncy of 2.78 Hz in the IMC control signal. Red arrows indicate odd harmonics, green arrows indicate even harmonics.
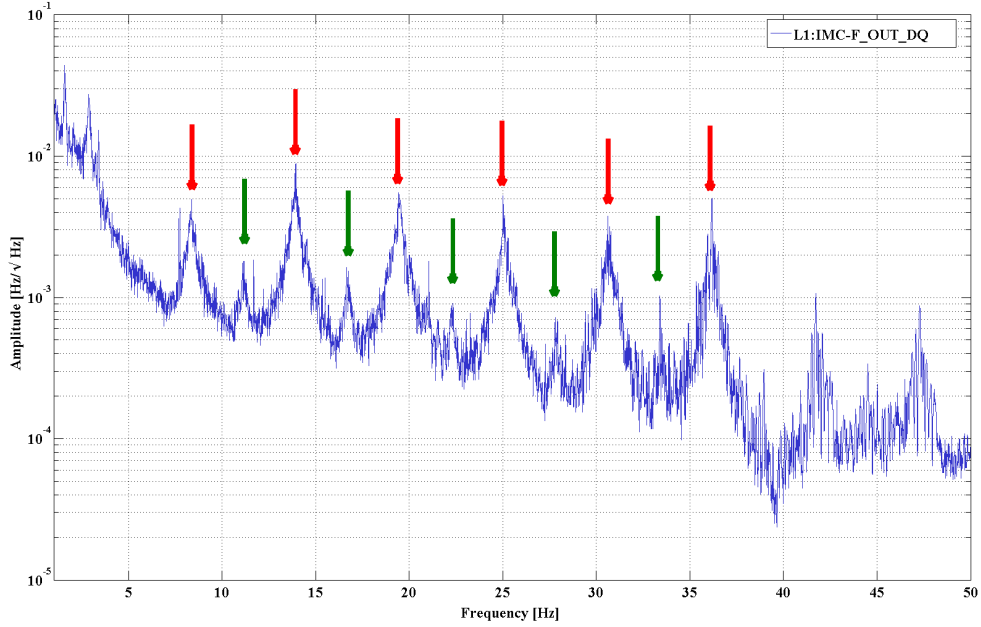
for a better way to look at the actual IMC error point during times of excess seismic motion instead of the control signal.

We also need to localize the source of the 2.78 Hz excitation. Why that specific frequency when the excess seismic noise is spread across a 1 - 5 Hz band? We think the source may be a vertical resonance of the triple pendulum suspension that houses the IMC optics being rung up by the excess motion.

We are also going to use the increasing full IFO uptime to figure out whether or not this upconversion noise is coupling downstream into critical cavities such as the recycling or arm cavities.

3.5   Conclusions

We found that injecting sinusoidal cavity motion into our input mode cleaner PDH model generates an error signal with non-linear spectral artifacts, specifically harmonics of the injection frequency, if the cavity motion exceeds the linear PDH range. For cavity motion that is symmetric about the locking point of the error signal, we

find that the error signal contains only odd harmonics. For asymmetric cavity motion we find both even and odd harmonics, where the odd harmonics are typically higher in amplitude. In such a case, the amplitude of the even harmonics increases as the DC offset from the nominal locking point increases, that is, as the cavity motion is more asymmetric.

Chapter 4

Online Detector Characterization

List of a whole bunch of ODC stuff. Descriptions and pictures of the LSC and ASC ODC and MEDM screens.

Bibliography

[1] J.A. Sidles and D. Sigg. Optical torques in suspended fabryperot interferometers. *Phys. Lett. A*, 354(3):167 – 172, 2006.

[2] Chris Mueller. The advanced ligo input mode cleaner dcc g1400096.

[3] E. D. Black. An introduction to Pound-Drever-Hall laser frequency stabilization. *Am. J. Phys.*, 69:79–87, 2001.

Curriculum Vitae

Title of Dissertation

    Detector Characterization of Advanced LIGO

Full Name

    Thomas J. Massinger

Place and Date of Birth

    Rochester, NY   July 22, 1989

Colleges and Universities,	Years attended and degrees
Utica College	2007–2011, B.S.
Syracuse University	2011–2016, Ph.D.

Publications

Major Department

    Physics